2007 SCEC ANNUAL REPORT

Helping to Evaluate and Improve the SCEC 3D Community Fault Model and Regional Seismicity Catalogs

Craig Nicholson

Marine Science Institute, University of California, Santa Barbara, CA 93106-6150

Project Description

The purpose of this project was to help evaluate 3D fault representations in the SCEC Community Fault Model (CFM) v.3.0 [*Plesch et al.,* 2006] using recently developed relocated earthquake catalogs [*Hauksson and Shearer*, 2005; *Shearer et al.,* 2005, 2006; *Lin et al.,* 2007]. This also included identifying and developing new and alternative representations for faults that are currently missing, or incompletely or inaccurately defined in the current CFM, as well as helping to distinguish between existing alternative fault models. The idea was to define a set of reference 3D fault surfaces (or calibration points) that exhibit a high degree of consistency between their surface and subsurface expressions (based on a wide range of independent data sets) such that the position of the fault at depth can be ascertained with a high degree of confidence. These 3D control points can then be used to help calibrate and evaluate the relocated earthquake catalogs. This is particularly critical in areas like the Imperial Valley and along the southern San Andreas and San Jacinto fault systems, where different velocity models and location procedures can significantly shift earthquake hypocenters relative to their mapped surface fault traces.

Activities:

1) A critical component of SCEC is understanding the pattern of crustal deformation in southern California. This includes accurate and complete descriptions of the 3D geometry and slip of subsurface faults, as well as documenting the nature of off-fault and non-elastic deformation that can contribute to the observed pattern of geodetic strain. For these reasons, we have been working to define and map both 3D fault surfaces [*e.g., Kamerling et al,* 2001, 2003; *Sorlien et al,* 2006; *Schindler et al.,* 2007] and dated stratigraphic reference horizons [*e.g., Kamerling et al.,* 1998; *Sorlien and Nicholson,* 2004]. If the original surface geometry is known or inferred, these dated reference horizons can be used to quantify the pattern of finite strain since deposition [*Kamerling et al.,* 1998; *Sorlien et al.,* 2000], and help model the geometry and slip rate of buried or blind faults [*Shaw and Suppe,* 1994*; Thibaut et al.,* 1996; *Seeber and Sorlien,* 2000; *Sorlien and Nicholson,* 2004]. If the paleo-depth of the reference surface is known, then estimates of the absolute vertical motion (uplift and subsidence) can also be determined. An excellent example of such a dated reference surface is the 1-Ma horizon, originally mapped by *Yeats* [1981] and subsequently modified and extended offshore by *Sorlien and Kamerling* [1998](**Figure 1**). This surface was originally deposited at mid-bathyal depths (~500 m). Onshore in the eastern Ventura Basin, it is now found at a depth of ~3.5 km (indicating an average basin subsidence rate of 3 mm/yr), while on Oak Ridge, it is at an elevation of ~1.5 km (indicating an uplift rate of about 2 mm/yr). By evaluating this and other deformed reference surfaces based on digital topography, surface mapping, seismic reflection, seismicity and subsurface well data, we developed a model for how non-elastic processes, such as subsidence, compaction and gravity-sliding, can affect the measurement of crustal strain and influence the 3D geometry, dynamic rupture and seismic hazard potential of basin-bounding faults in southern California [*Nicholson et al.,* 2007].

2) As part of an on-going collaboration with the USGS and CSU Bakersfield [*Fisher et al.,* 2005; *Schindler et al.,* 2006], we have continued to map 3D fault surfaces and stratigraphic reference horizons in the offshore California Continental Borderland [*Schindler et al.,* 2007]. This mapping effort is based primarily on extensive grids of newly released industry marine multichannel seismic (MCS) reflection data that were made available through a collaboration of the SCEC Borderland Working Group and the USGS *[Nicholson et al.,* 2004; *Childs and Hart,* 2004]. Digital data and navigation files are now accessible through the USGS National Archive of Marine Seismic Surveys website (http://walrus.wr.usgs.gov/NAMSS/). Our results include documenting the pattern of uplift, subsidence, and basin inversion associated with the rifting of the continental margin, offshore basin development and subsequent reactivation of the plate boundary in transpression. We also mapped several 3D surfaces of Quaternary active faults, including active strands of the Ferrelo, East Santa Cruz Basin, Catalina Ridge, Channel Islands Thrust and Malibu Coast-Dume faults (**Figure 2**)[*Schindler et al.,* 2007]. Digital 3D fault representations of these active fault strands, mapped to depths of ~6 km, were recently provided to SCEC for inclusion in the SCEC Community Fault Model (CFM)[*Plesch et al.,* 2007].

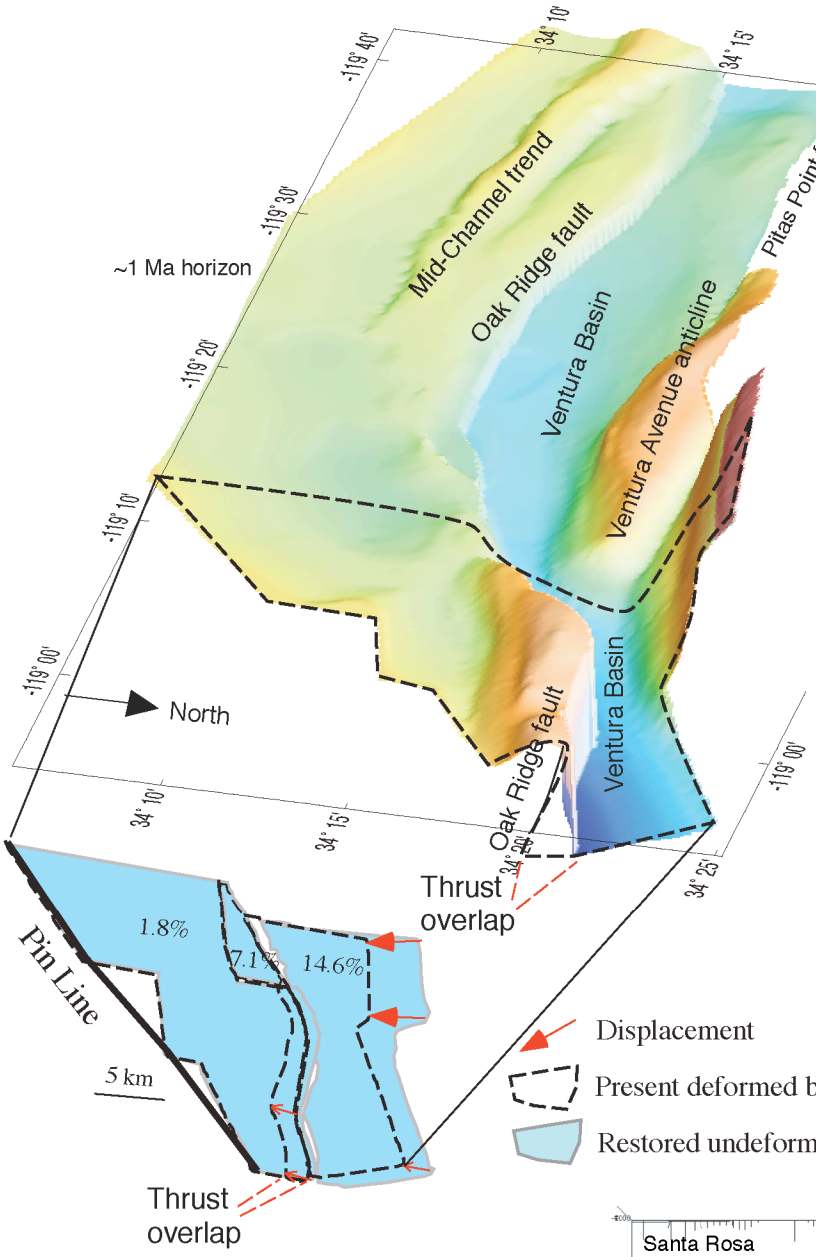

Figure 1. Oblique 3D GOCAD view to the west of 1-Ma horizon mapped by Yeats (1981) and subsequently modified and extended by Sorlien and Kamerling (1998). This horizon documents the cumulative finite strain, and overall pattern of uplift and subsidence since deposition. Inset below shows 3D restoration of the map foreground outlined by the heavy dashed line (Kamerling et al., 1998). Blue-filled shapes show restored outlines of present deformed blocks and the %-strain each block accommodated by folding; red arrows show displacements with respect to the pin line. Such 3D surfaces and other data sets were used to model how non-elastic processes, such as subsidence, compaction and gravity-sliding, can affect measurements of crustal strain and influence the 3D geometry, dynamic rupture and seismic hazard potential of basin-bounding faults in southern California (Nicholson et al., 2007).

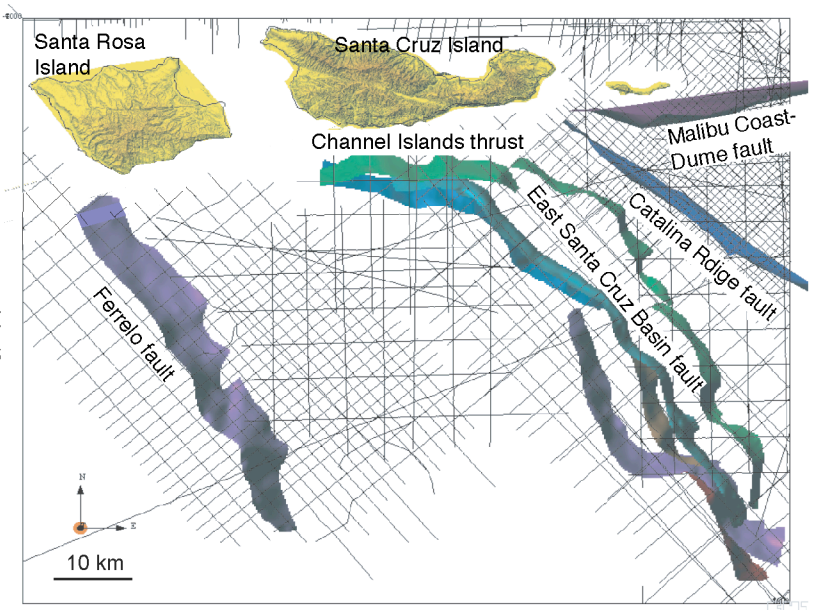

Figure 2. Map view of 3D fault surfaces of Quaternary active faults in the offshore Northern California Borderland (Schindler et al., 2006, 2007). These 3D fault models include active strands of the Ferrelo fault, the East Santa Cruz Basin fault, the Catalina Ridge fault, the Channel Islands Thrust fault and the Malibu Coast-Dume fault. The 3D fault surfaces, developed in collaboration with Chris Sorlien and our student Sarah Schindler, are based on extensive grids of recently released industry seismic reflection data (black lines) available from the USGS NAMSS website. The 3D fault surfaces shown here, mapped to depths of ~6 km, have been recently provided to the SCEC CFM.

3) Accurately characterizing the 3D geometry of active subsurface faults is particularly important for any number of SCEC activities, including resolving geodetic strain data into fault slip, evaluating fault stress or stress changes associated with fault slip, and estimating ground motions from dynamic rupture propagation. For these reasons, a considerable effort within SCEC was focused on developing both the SCEC 3D Community Fault Model (CFM) [*e.g., Plesch et al.,* 2005, 2006, 2007] and improved relocated earthquake catalogs [*e.g., Hauksson and Shearer,* 2005; *Shearer et al.,* 2005, 2006; *Lin et al.,* 2007]. These efforts though are not yet complete. Both CFM and the earthquake catalogs need to be critically evaluated to identify missing, incomplete or inaccurate fault representations, and to validate location procedures, velocity models, and the reliability of the resulting earthquake hypocenters. Such efforts are fundamental to SCEC's primary research priorities if we are to successfully discriminated between on-fault and off-fault earthquakes, and accurately characterize the seismic behavior, subsurface geometry and moment-release rate of major mapped faults.

As part of this on-going evaluation process, a number of SCEC researchers have conducted various statistical studies to associate southern California seismicity with CFM fault representations [*Hauksson et al.,* 2004, 2005; *Powers and Jordan,* 2005, 2006; *Woessner and Hauksson,* 2006]. The problem, however, is that CFM fault representations and earthquake catalogs are often not independent, and a number of these comparison tests focused on *relative*, rather than *absolute* location differences. In addition, the statistical tests typically evaluated only the proximity of a single event (hypocenter) to a modeled fault, and thus did not incorporate or evaluate the aggregate alignment of multiple hypocenters or nodal planes in terms of their consistency with each other or to the local orientation of the CFM fault. Thus, a considerable amount of valuable spatial information was lost in using such statistical tests. The issue then becomes what to do when significant discrepancies exist between the fault representation in CFM and the distribution of hypocenters that are believed to be associated with the fault.

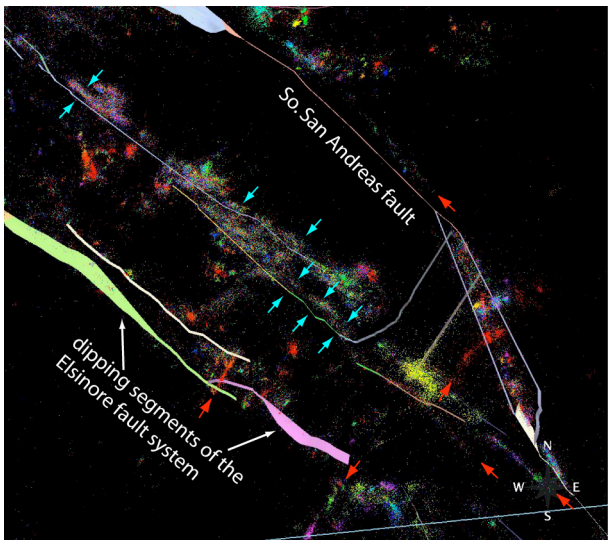

Figure 3. Map view of CFM v3.0 [*Plesch et al.,* 2006] and relocated hypocenters using a 3D velocity model [*Hauksson,* 2000] in the area of the southern San Jacinto and southern San Adreas fault zones. Note systematic discrepancies between mapped 3D fault surfaces and earthquake locations (blue arrows) at depth in certain areas, and the presence of linear earthquake alignments along active faults not yet represented in the preferred CFM v3.0 (red arrows). Subparallel trend along Southern San Andreas fault may be the subsidiary Hidden Springs fault [*Williams et al.,* 1990], not currently accounted for in paleoseismic studies [*Bennett et al.,* 2004]. Our project has been working to evaluate and improve CFM, to develop new 3D fault representations for the major faults that correlate better with the seismicity at depth, and to incorporate these and other missing fault structures in CFM, together with the SCEC CFM Working Group.

As **Figure 3** shows, comparison of CFM faults with earthquake relocations using a 3D model [*Hauksson,* 2000] reveal several such discrepancies. First, there are distinct linear trends in earthquake epicenters (red arrows) that represent active near-vertical fault segments missing in CFM. Second, systematic discrepancies exist between 3D fault surfaces of major mapped faults as represented in CFM and earthquake hypocenters in certain areas (blue arrows) [*Nicholson,* 2006]. In many of these areas where discrepancies occur, the fault model was projected to depth from the surface trace assuming the strike-slip fault was vertical. The question is thus to what extent are these observed shifts between the fault model and the hypocenters the result of: a) incorrect extrapolation or projection of mapped surface fault traces to depth; b) earthquake mislocation owing to velocity models or location procedures used; or possibly c) existence of a previously unidentified active, blind sub-parallel fault strand.

To resolve these issues and the possible source of the observed offsets, we have been evaluating the relative hypocentral locations between the various earthquake catalogs, and documenting the segments of major CFM faults that exhibit some of the largest offsets with seismicity in order to produce improved 3D fault representations for CFM [*Nicholson,* 2006; *Nicholson et al.,* 2007]. The idea is to identify and establish a set of calibration control points, such as reference 3D fault surfaces and principal earthquake hypocenters and focal mechanisms, which based on their internal kinematic consistency and other independent criteria can be used to define the orientation and position of active fault segments at depth. These control points can then provide a

reference framework within which to further calibrate and evaluate CFM and the new earthquake catalog, and thus provide a means to independently check trade-offs in model changes to either 3D fault surfaces or earthquake locations.

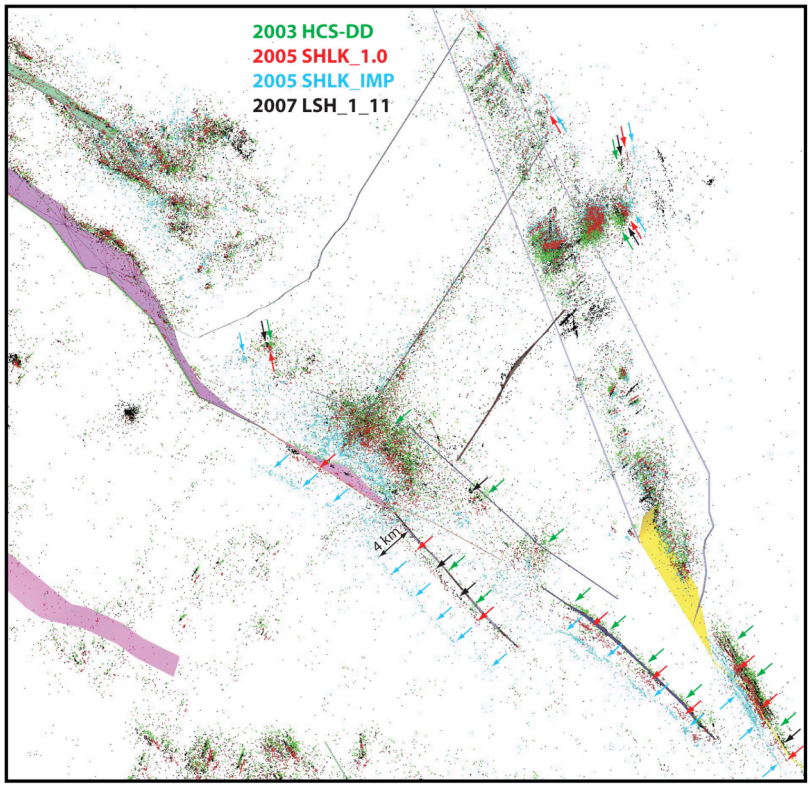

Figure 4. Effects of different location procedures and velocity models on systematic offsets (arrows) of earthquake epicenters from mapped CFM fault models for the Salton Trough region. Different colors represent different seismicity catalogs including double-difference locations starting from 3D velocity model hypocenters (green) [*Hauksson et al.,* 2003], cross correlation locations using regional 1D velocity models (red) and a 1D model specific to the Imperial Valley area (blue) [*Shearer et al.,* 2005], and the most recent relocations combining cross correlation, refined cluster analysis and 3D P- and S-velocity models (black)[*Lin et al.,* 2007]. For reference, the blue epicenters are displaced up to 4 km (double arrow) from the mapped surface traces of the Superstition Mountain and Superstition Hills faults. To the SW, events are displaced between catalogs westward from green to black to red to blue, while to the NE this pattern is reversed and events are shifted eastward.

This problem of systematic discrepancies between well located earthquake hypocenters and CFM faults is particularly critical in areas like the Imperial Valley and along the southern San Andreas and San Jacinto fault systems, where different velocity models and location procedures can significantly shift earthquake hypocenters relative to their mapped surface fault traces (**Figure 4**) [*Nicholson et al.,* 2007]. For example, none of the existing earthquake catalogs shown in **Figure 4** actually locate the 1987 M6.6 Superstition Hills main shock and aftershocks directly beneath the mapped surface trace of the Superstition Hills fault, as would be expected from many of the earthquake focal mechanisms that indicate predominantly right-slip on a vertical strike-slip fault. Given that different catalogs can systematically shift these events by different amounts and those catalogs using the lowest velocities are typically displaced the farthest, this suggests a problem in the location procedures or velocity models that may be overcompensating for the low-velocity sediments in the Imperial Valley.

Additional examples of this problem are shown for the southern San Andreas fault in the northern Coachella Valley (**Figures 5&6**) and for the central Elsinore fault (**Figures 7&8**). These figures show maps and cross sections of relocated hypocenters (gold circles) [*Lin et al.,* 2007], single focal mechanism nodal planes (projected curves of their intersection with the focal sphere and colored according to slip vector) [*Hauksson et al.,* 2003], and in the case of the GOCAD volumes, relocated hypocenters and CFM fault surfaces. In the example from the northern Coachella Valley (inset, **Fig.5**), the CFM fault representations for the NNE-dipping Garnet Hill fault (GHF, blue) and Banning fault (BF, gold) merge at shallow depth and become more steeply dipping to coalesce with an inferred SW-dipping Mission Creek fault (MCF, red). However, the actual earthquake hypocenter and nodal plane alignments (**Fig.6**, Cross Section 1) show that the Garnet Hill and Banning faults are most likely sub-parallel to depths of about 10 to 12 km (as are other active fault segments) and become less steeply dipping, rather than more steeply dipping with depth [*Nicholson,* 1996; *Nicholson et al.,* 2007. Independent data sets, including gravity, sediment thickness and water well data, confirm that the Garnet Hill and Banning faults are sub-parallel and near vertical in the upper 2 to 3 km in the northern Coachella Valley [*Langenheim et al.,* 2005; *Tyley,* 1974]. Gravity modeling [*Griscom and Jachens,* 1990] also suggest that the Mission Creek fault is moderately NE-dipping, as is shown by the seismicity data farther SE along the fault (**Fig.6**, Cross Section 2). This implies that the alternative fault representation for the Mission Creek fault in CFM that is NE-dipping is the preferred fault

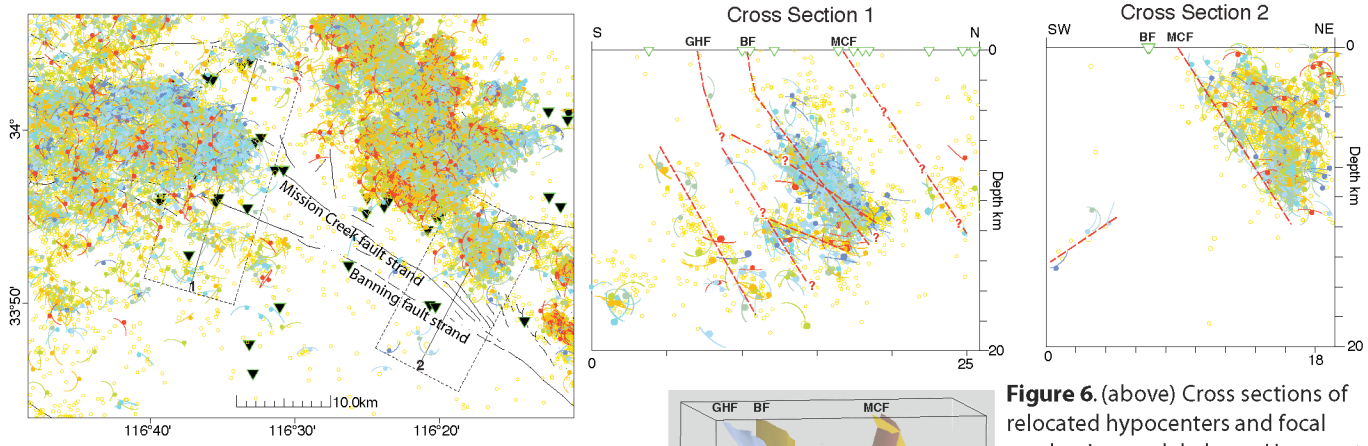

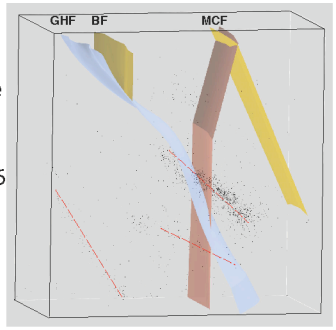

Figure 5. Relocated epicenters [Lin et al., 2007] and upper-hemisphere projected single nodel planes from earthquake focal mechanisms [Hauksson, 2003] for the northern Coachella Valley region. Large earthquakes that occurred in 1948 (M6.3 Desert Hot Springs) and 1986 (M6.0 North Palm Springs) [Nicholson and Lees, 1992; Nicholson, 1996] along the Banning strand of the southern San Andreas fault indicate that the fault likely dips 50° to 70°NE at depth. Gravity modeling also suggests that the Mission Creek fault (MCF) is moderately NE-dipping in this area. Independent data sets, including gravity, sediment thickness and water-well data, indicate that the Garnet Hill (GHF) and Banning faults (BF) are sub-parallel and steeply dipping in the upper 2 to 3 km in the northern Coachella Valley. Together with the alignment of relocated hypocenters and focal mechanism nodal planes, this suggests a complex 3D geometry and fault interaction with these active strands of the southern San Andreas fault that is different from that typically shown in CFM. The GOCAD volume at right shows relocated hypocenters and fault representations currently in CFM. It is similar to Cross Section 1 above it. Clearly, there is a discrepancy between the orientation of faults at depth in CFM and that defined by seismicity.

Figure 6. (above) Cross sections of relocated hypocenters and focal mechanism nodel planes. Hypocentral and nodal plane alignments, together with other subsurface data suggest that, in Cross Section 1, the Banning fault (BF) is non-planar to listric, is moderately dipping (45°-50°) at depth, and may be multi-stranded. The Garnet Hill fault (GHF) is equally complicated, is likely sub-parallel and may merge with the Banning at different depths depending on the interpretation. Farther to the SE (Cross Section 2), the Mission Creek fault (MCF) appears to act as a moderately NE-dipping delimiter to the microseismicty at depth. Other blind subsurface faults are evident that are not currently in CFM.

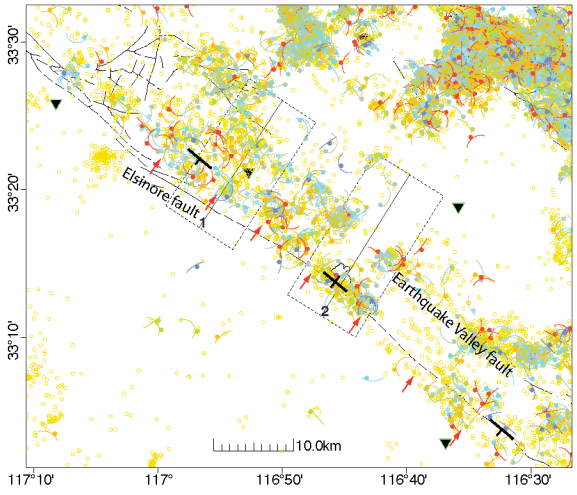

Figure 7. Relocated epicenters [Lin et al., 2007] and upper-hemisphere projected focal mechanism nodel planes [Hauksson, 2003] for the central Elsinore fault zone [Hull and Nicholson, 1992]. Epicenters most likely associated with the main fault are displaced from east of the surface trace to west of the surface trace SE along the fault (red arrows), suggesting a possible systematic change in dip from slightly NE to vertical to slightly SW dipping. However, the alignment of hypocenters and nodel planes (Fig.8) suggest that the fault at depth is always SW-dipping to vertical along this section. The sub-parallel Earthquake Valley fault (EVF) is typically sub-vertical to NE-dipping, but in CFM it is only shown as vertical.

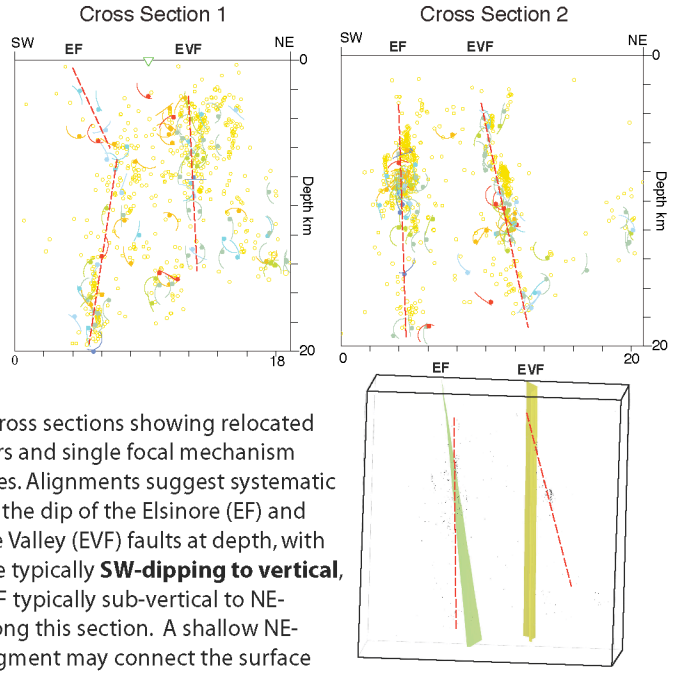

Figure 8. Cross sections showing relocated hypocenters and single focal mechanism nodel planes. Alignments suggest systematic changes in the dip of the Elsinore (EF) and Earthquake Valley (EVF) faults at depth, with the Elsinore typically **SW-dipping to vertical**, and the EVF typically sub-vertical to NE-dipping along this section. A shallow NE-dipping segment may connect the surface trace to the deep Elsinore fault in Cross Section 1. This contrasts with the current 3D fault representations for these faults in CFM that has the EVF always vertical (gold) and the **Elsinore always steeply NE-dipping** (green). Lower figure is the GOCAD volume similar to that shown in Cross Section 2, with the projected planar dips from Cross Section 2 shown as dashed red lines. This suggests that projections of near-surface dips to depth assuming constant (often vertical) dips and constant dip directions may not be a reliable method of estimating the fault orientation at depth.

model, and that alternative 3D models for the Garnet Hill and Banning faults that are more complex, sub-parallel and less steeply dipping with depth need to be included in CFM. Such alternative 3D fault geometry would have significant implications for how dynamic earthquake ruptures may propagate or stresses would be resolved along this section of the southern San Andreas fault system.

In the example from the central Elsinore fault zone, earthquake epicenters tend from being displaced NE of the fault to SW of the fault (red arrows, **Fig.7**) suggesting that the fault may change dip along strike to being NE-dipping to SW-dipping. However, cross section views of the earthquake hypocenters and focal mechanism nodal planes (**Fig.8**, Cross Sections 1&2) show that at depth, the fault actually changes from SW-dipping to near vertical to back to being SW-dipping [*Hull and Nicholson,* 1992; *Nicholson et al.,* 2007]. The NE offset in Cross Section 1 appears to be the result of a shallow NE-dipping segment that connects the surface trace of the Elsinore fault with its deeper, blind SW-dipping segment. In CFM, however, the Elsinore fault is always NE-dipping along this fault segment (**Fig.3**). For the adjacent sub-parallel Earthquake Valley fault (EVF), hypocenter and nodal plane alignments indicate a fault that changes dip from steeply dipping to NE-dipping, while in CFM, this fault segment is currently always vertical.

These examples demonstrate that major strike-slip faults in southern California, like the Elsinore, San Jacinto and southern San Andreas faults, often exhibit multiple fault strands that are sub-parallel throughout the seismogenic zone, and change dip and dip direction along strike and with depth (**Figs.6&8**)[*e.g., Hull and Nicholson,* 1992; *Magistrale and Rockwell,* 1996; *Nicholson,* 1996; *Sanders and Magistrale*, 1997; *Nicholson et al.,* 2007]. As a result, I have been developing alternative 3D fault models for these faults, and relaxing the assumption that strike-slip faults are necessarily vertical, or exhibit a constant dip and dip direction. New fault representations for the Anza, Borrego, and Coyote Creek segments of the San Jacinto fault, northern segment, southern segment, and extension of the Superstition Mountain fault towards Cerro Prieto, and Weinert-El Centro extension-Superstition Hills [*Magistrale*, 2002] were added or modified to conform better to earthquake hypocenters and lineations at depth [*Nicholson,* 2006; *Nicholson et al.,* 2007]. Westmorland and Sawtooth Range cross faults [*Nicholson et al.,* 1986] and the possible NE-dipping Hidden Springs fault (**Fig.3**)[*Williams et al.,* 1990] adjacent to the southern San Andreas fault were also developed. These and other representations of digital 3D fault surfaces have been provided to CFM, but clearly more work still needs to be done. This includes development of new alternative 3D fault representations for the active strands of the Elsinore and southern San Andreas fault systems that better match the observed hypocenter and focal mechanism alignments at depth (**Figs.6&8**). This work is currently in progress.

Recent SCEC Project Reports and Publications

Nicholson, C., C.C. Sorlien, S. Hopkins, J. Kennett et al., Combining high-resolution climate studies and tectonics: Imaging complex folding in 4-dimensions above active blind faults, *International Workshop on Comparative Studies of the North Anatolian fault (Northwest Turkey) and the San Andreas fault (Southern California) Abstracts*, p. 21-22, Istanbul, Turkey, August 14-18 (2006).

Nicholson, C. Continuing to Build and Evaluate the SCEC 3D Community Fault Model and Deformed Reference Surface Libraries, *2006 SCEC Annual Report,* n.06036, 7 pp (2007).

Nicholson, C., M.J. Kamerling, C.C. Sorlien, T.E. Hopps and J.-P. Gratier, Subsidence, compaction and gravity-sliding: Implications for 3D geometry, dynamic rupture and seismic hazard of active basin-bounding faults in southern California, *Bulletin of the Seismological Society of America*, **v.97**, n.5, p.1607-1620 (2007).

Nicholson, C., A. Plesch. G. Lin, P. Shearer and E. Hauksson, Evaluating SCEC 3D Community Fault Model v3.0 and Regional Seismicity Catalogs, *2007 SCEC Annual Meeting Proc. & Abstracts*, **XVII**, p.149 (2007).

Plesch, A., J. Shaw et. al., Community Fault Model (CFM) for Southern California, *Bulletin of the Seismological Society of America,* **v.97**, n.6, p.1793–1802, doi: 10.1785/0120050211 (2007).

Schindler, C.S., C. Nicholson and C. Sorlien, Imaging and mapping active 3D fault geometry in the California Continental Borderland, *2006 SCEC Annual Meeting Report,* **XVI**, p.157-158 (2006).

Schindler, C.S., C. Nicholson and C. Sorlien, 3D Fault Geometry and Offshore Basin Evolution in the Northern Continental Borderland, *2007 SCEC Annual Meeting Proceedings and Abstracts*, **XVII**, p.171 (2007).

Schindler, C.S., C. Nicholson and C. Sorlien, 3D Fault Geometry and Basin Evolution in the Northern Continental Borderland Offshore Southern California, *Eos (Trans. AGU)*, **v.88**, n.52, abstr. T32A-1100 (2007).

References

Bennett, R.A., A.M. Friedrich and K.P. Furlong, Codependent histories of the San Andreas and San Jacinto fault zones from inversion of fault displacement rates, *Geology*, **v.32**, n.11, p.961-964, 2004.

Childs, J.R and P.E. Hart, National archive of marine seismic surveys (NAMSS): U.S. Geological Survey program to provide new access to proprietary data, *Eos (Trans. AGU)*, **v.85**, n.47, NG43A-0441, 2004.

Fisher, M., V. Langenheim, C. Sorlien, C. Nicholson, and R. Sliter, Active fault deformation along the southern boundary of the Western Transverse Ranges Province, Pt. Dume to Northern Channel Islands, Southern CA, *Eos (Transactions of AGU)*, **v.86**, n.52, abstract T51D-1362 (2005).

Griscom, A. and R.C. Jachens, Crustal and lithospheric structure from gravity and magnetic studies, in *The San Andreas Fault System, California*, R.E. Wallace, ed., *US Geological Survey Professional Paper 1515*, p. 239-260 (1990).

Hauksson, E. and P. Shearer, Southern California hypocenter relocation with waveform cross-correlation; Part 1, Results using the double-difference method, *Bull. Seismol. Soc. Am.,* **v.95**, n.3, p.893-903, 2005.

Hauksson, E., Crustal structure and seismicity distribution adjacent to the Pacific and North American plate boundary in southern California, *J. Geophys. Res.,* **v.105**, n.B6, p. 13,875-13,899 (2000).

Hauksson, E., R. Wesson, P. Shearer and J. Shaw, Associating southern California seismicity with faults using Bayesian inference, *2005 SCEC Annual Meeting Proceedings and Abstracts*, **XV**, p.132, 2005.

Hauksson, E., R. Wesson, P. Shearer, J. Shaw, Associating southern California seismicity with mapped late-Quaternary faults, *2004 SCEC Annual Meeting Proceedings and Abstracts*, **XIV**, p.105-106.

Hauksson, E., W-C. Chi, and P. Shearer, Comprehensive waveform cross-correlation of southern California seismograms: Part 1. Refined hypocenters obtained using the double-difference method and tectonic implications, *Eos (Trans. AGU)*, **v.84**, 2003.

Hudnut, K., L. Seeber and J. Pacheco, Cross-fault triggering in the November 1987 Superstition Hills earthquake sequence, southern California, *Geophys. Res. Lett.*, **16**, p. 199–202, 1989.

Hull, A.G. and C. Nicholson, Seismotectonics of the Northern Elsinore fault zone, southern California, *Bulletin Seismological Society of America*, **v.82**, p. 800-818 (1992).

Kamerling, M.J., C.C. Sorlien, and C. Nicholson (1998), Subsurface faulting and folding onshore and offshore of Ventura basin: 3D map restoration across the Oak Ridge fault, *SCEC 1998 Annual Meeting Report,* p.68-69.

Kamerling, M.J., C.C. Sorlien, R. Archuleta and C. Nicholson, Three dimensional geometry and interaction of faults and structures along the northern margin of the Santa Barbara Channel, California, *97th Cordilleran Section–Geol. Soc. Am. & Pacific Section–AAPG Meeting*, Los Angeles, CA, p.A-41 (2001).

Kamerling, M.J., C.C. Sorlien and C. Nicholson (2003), 3D development of an active oblique fault system, northern Santa Barbara Channel, California, *Seismol. Res. Lett.,* **v. 74**, n.2, p. 248.

Langenheim, V.E, R.C. Jachens, J.C. Matti, E. Hauksson, D.M. Morton, and A.Christensen, Geophysical evidence for wedging in the San Gorgonio Pass structural knot, southern San Andreas fault zone, southern California, *Geo. Soc. Am. Bull.*, **v.117**, n.11/12, p.1554-1572, 2005.

Lees, J. M., Geotouch: Software for Three and Four-Dimensional GIS in the Earth Sciences, *Computers & Geosciences*, 1999.

Lin, G., P. M. Shearer, and E. Hauksson, Applying a three-dimensional velocity model, waveform cross-correlation, and cluster analysis to locate southern California seismicity from 1981 to 2005, *J. Geophys. Res.*, **v.112**, n.B12, 14 pp, B12309, doi:10.1029/2007JB004986, 2007.

Lisowski, M. and J.C. Savage, Deformation associated with the Superstition Hills, California, earthquakes of November 1987 (abstract), *Seismol. Res. Lett.,* **59**, 35 (1988).

Magistrale, H. and T.K. Rockwell, The central and southern Elsinore fault zone, Southern California *Bulletin of the Seismological Society of America*, **v.86**, n.6, p.1793-1803, 1996.

Magistrale, H., The relation of the southern San Jacinto fault zone to the Imperial and Cerro Prieto faults, *Geo. Soc. Am. Spec. Paper,* **v.365,** p. 271-278, 2002.

Nicholson, C., Seismic behavior of the San Andreas fault in the Northern Coachella Valley, California: Comparison of the 1948 and 1986 earthquake sequences, *Bulletin of the Seismological Society of America,* **v.86**, n. 5, p. 1331-1349 (1996).

Nicholson, C. and M.J. Kamerling (1998), Reliability of 2D kinematic fold models to infer deep fault structure in the western Transverse Ranges, California, *Proceedings of the NEHRP Conference and Workshop on the Northridge, California Earthquake,* **v. II**, p. 299–306.

Nicholson, C. and J.M. Lees, Travel-time tomography in the northern Coachella Valley using aftershocks of the 1986 M_L 5.9 North Palm Springs earthquake, *Geophysical Research Letters*, **19**, p. 1-4 plus cover (1992).

Nicholson, C. and L. Seeber, Evidence for contemporary block rotation in strike-slip environments: Examples from the San Andreas fault system, southern California, in *Paleomagnetic Rotations and Continental Deformation,* C. Kissel and C. Laj, eds., Kluwer Academic Publishers, p. 247-280 (1989).

Nicholson, C., L. Seeber, P. Williams and L.R. Sykes. Seismic evidence for conjugate slip and block rotation within the San Andreas fault system, southern California, *Tectonics*, **5**, p. 629-648 (1986).

Nicholson, C., C.C. Sorlien and J.R Childs, GENII: A developing consortium to archive and use industry data to evaluate plate boundary structure, deformation and evolution, *16th Annual IRIS Workshop*, Tucson, AZ (2004).

Plesch, A., J. Shaw and the SCEC USR Focus Group members, Community Fault Model (CFM) Version 3.0 and related models for southern California, *2006 SCEC Annual Meeting Proceedings and Abstracts*, **XVI**, p.144-145, 2006.

Plesch, A., J.H. Shaw, others and the SCEC CFM Working Group, The Community Fault Model Version 2.5 and associated models, *2005 SCEC Annual Meeting Proceedings and Abstracts*, **XV**, p.168-169, 2005.

Powers, P. and T. Jordan, Seismicity rate vs distance from strike-slip faults in Southern California, *2005 SCEC Annual Meeting Proceedings and Abstracts*, **XV**, p.171, 2005.

Powers, P. and T. Jordan, Spatial constraints on seismicity distributions around California faults, *2006 SCEC Annual Meeting Proceedings and Abstracts*, **XVI**, p.145-146, 2006.

Sanders, C. and H. Magistrale, Segmentation of the northern San Jacinto fault zone, Southern California, *Journal of Geophysical Research,* vol.102, no.B12, pp.27,453-27,467, 1997.

Seeber, L, and Sorlien, C. C., 2000, Listric thrusts in the western Transverse Ranges, California, Geological Society of America Bulletin, v. 112, p. 1067-1079

Shaw, J.H. and J. Suppe, Active faulting and growth folding in the eastern Santa Barbara Channel, California, *Geol. Soc. Am. Bull.,* **v. 106,** p. 607–626, 1994.

Shaw, J.H. and P.M. Shearer, An elusive blind-thrust fault beneath metropolitan Los Angeles, *Science,* **v.283**, p. 1,516-1,518, 1999.

Shearer, P., E. Hauksson and G. Lin, Southern California hypocenter relocation with waveform cross-correlation, Part 2 Results using Source-specific station terms and cluster analysis, *Bull. Seismol. Soc. Am.,* **v.95**, n.3, p.904-915, 2005.

Shearer, P., G. Lin and E. Hauksson, Improved locations for southern California earthquakes from 1981 to 2005, *2006 SCEC Annual Meeting Proceedings and Abstracts*, **XVI**, p.161, 2006.

Sorlien, C.C., J.P. Gratier, B.P. Luyendyk, J.S. Hornafius and T.E. Hopps, 2000, Map restoration of folded and faulted late Cenozoic strata across the Oak Ridge fault, onshore and offshore Ventura basin, California, *Geological Society of America Bulletin*, **v. 112**, p. 1080-1090

Sorlien, C.C. and M.J. Kamerling, 1998, Fault displacement and fold contraction estimated from unfolding of Quaternary strata onshore and offshore Ventura basin, California. *U.S. Geological Survey NEHRP Final Technical Report 97-GR-03085*, 16 pp., digital map scale 1/100,000.

Sorlien, C. C., M. J. Kamerling, L. Seeber, and K. G. Broderick (2006), Restraining segments and reactivation of the Santa Monica–Dume–Malibu Coast fault system, offshore Los Angeles, California, *J. Geophys. Res.*, **111**, B11402, doi:10.1029/2005JB003632.

Sorlien, C.C. and C. Nicholson, Suggestions for SCEC3: Providing a Unified Structural Representation for Active Faults, Folds, and Basin Development, *2004 SCEC Annual Meeting* **XIV**, p.162-163, Palm Springs, CA (2004).

Thibaut, M., J.P. Gratier, M. Léger, and J.M. Morvan (1996). An inverse method for determining three-dimensional fault geometry with thread criterion: application to strike-slip and thrust faults, *J. Structural Geol.,* **v.18,** p. 1127–1138.

Tyley, S.J., Analog model study of the ground-water basin of the upper Coachella Valley, California, *U.S. Geological Survey Water-Supply Paper 2027*, 77 p. (1974).

Williams, P., L. Sykes, C. Nicholson, L. Seeber. Seismotectonics of the Easternmost Transverse Ranges California: Relevance for seismic potential of the San Andreas fault, *Tectonics,* **9,** 185-204 (1990).

Woessner, J. and E. Hauksson, Associating southern California seismicity with late-Quaternary faults: Implications for seismicity parameters, *2006 SCEC Annual Meeting Proc. Abstr.*, **XVI**, p.181, 2006.

Yeats, R. S., 1981, Deformation of a 1 Ma Datum, Ventura Basin, California: *U. S. Geological Survey, Technical Report,* Contract No. 14-08-0001-18283.